Supplementary Material

Molecular understanding of Charge Effect on Desalination Performance in Lamellar MoS_2 Membranes

Junhui Yao [a], Chen Chen [a], Jing Zhang [a], Li Zhang *[a], Wei Zhang [a], Jia-Wei Shen *[b] Lijun Liang [c]

[a] Department of Chemistry, Key Laboratory of Surface & Interface Science of Polymer Materials of Zhejiang Province. Zhejiang Sci-Tech University, Hangzhou, 310018, People's Republic of China

[b] School of Pharmacy, Hangzhou Normal University, Hangzhou, 310016, People's Republic of China

[c] College of Life Information Science and Instrument Engineering, Hangzhou Dianzi University, Hangzhou 310018, People's Republic of China

∗ Corresponding authors.

E-mail addresses: lizhang@zstu.edu.cn (L. Zhang), shen.jiawei@hotmail.com (J.-W. Shen)

1.The definition of interlayer spacing and pore width

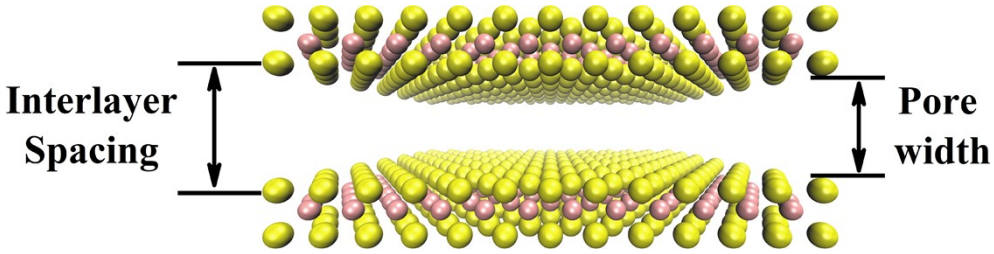

The interlayer spacing (short for H) refers to the distance between the mass center of the lower and upper S atoms in separate MoS_2 layers. The interlayer spacing of MoS_2 nanosheets in our work was set to be 0.8 nm, 0.9 nm, 1.0 nm, 1.1 nm, and 1.3 nm.

The pore width refers to the distance by taking away the radius of S atoms (about 1.0 Å, short for R_S) from the interlayer spacing (H). Hence, the pore width in our work was 0.6 nm, 0.7 nm, 0.8 nm, 0.9 nm, and 1.1 nm, separately. In the revised manuscript, pore width was used to describe and analyze relevant contents.

$$Pore\ width = H - 2R_S$$

2. The calculation of water flux rate and ions rejection rate

As shown in Fig. S2, a large number of water molecules pass through the membrane at the beginning of the simulation. The amount of water molecules passing through the membrane to the right side increases gradually as time goes on. The trajectories of each simulation system were selected to analyze their water flux rate and ions rejection rate after all the system are steady. The calculation formulas [1] are listed as follows:

$$water\ flux\ rate = \frac{N_{t_2} - N_{t_1}}{t_2 - t_1} \quad (1)$$

$$salt\ rejection\ \% = \frac{C_{initial} - C_{pass}}{C_{initial}} \times 100\%$$

$$C_{initial} = \frac{T_{ion}}{T_{H_2O}}, \quad C_{pass} = \frac{P_{ion}}{P_{H_2O}} \quad (2)$$

where N_{t_1} and N_{t_2} are the number of water molecules passing through the right side of the lamellar MoS_2 membrane at time t_1 and t_2, respectively. T_{H_2O} and T_{ion} represent the number of water molecules and Na^+/Cl^- in the NaCl solution on the left side of the MoS_2 at the initial time. The water flux was recalculated by dividing water flux rate to the surface area of the membranes, the unit of water flux in the revised manuscript is

$L \cdot cm^{-2} \cdot h^{-1}$.

3. Supplementary Figures

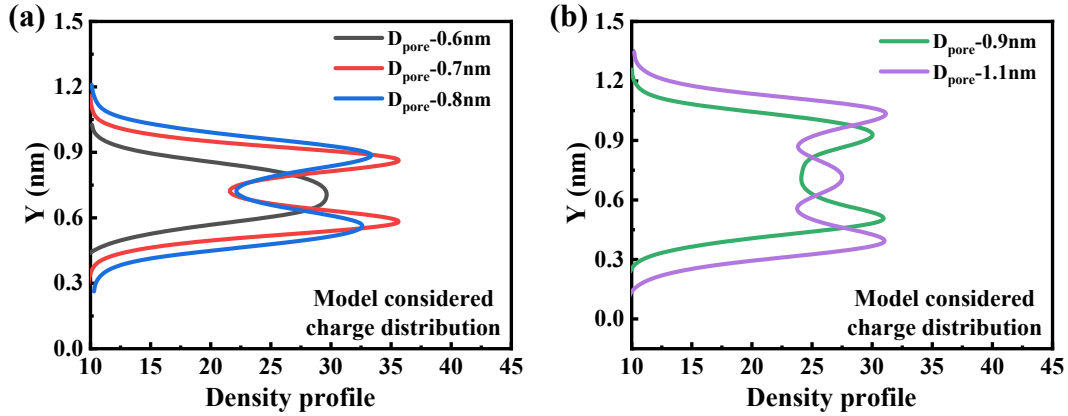

Fig. S1 The density distribution profiles for water molecules along *y*-direction in the MoS_2 membranes described by model considered charge distribution with different pore width (0.6 nm-1.1 nm).

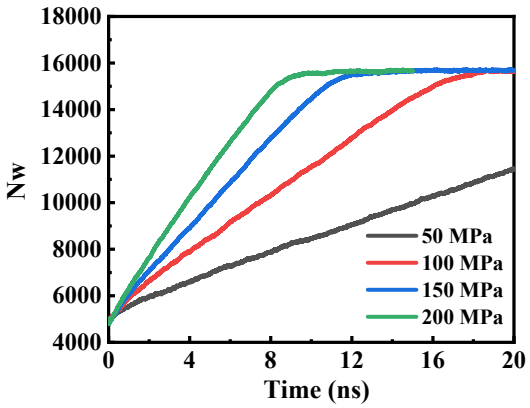

Fig. S2 The number of water molecules transferred from NaCl solution to pure water in the MoS_2 membrane described by model considered charge distribution under different pressures at different simulation time.

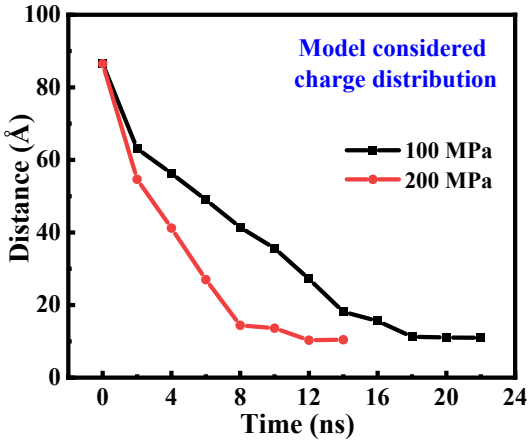

Fig. S3 The distance between graphene-1 sheet and MoS_2 membrane versus simulation time under different external pressures in the MoS_2 membrane described by model considered charge distribution.

At the beginning of the simulation, the distance between graphene-l sheet and MoS_2 nanosheets was about ~87 Å, and it was about ~10 Å at the end of the simulation.

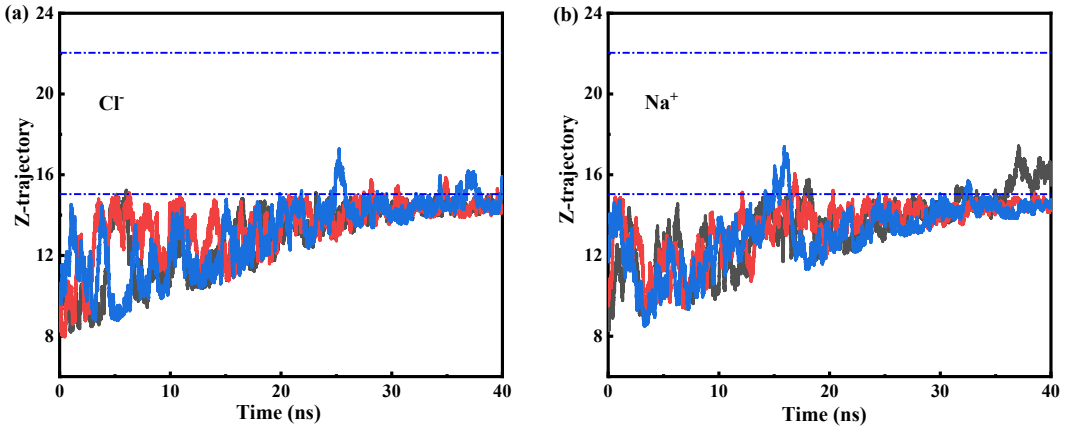

Fig. S4 The trajectories of the randomly selected (a) Cl^- ions and (b) Na^+ ions passing through the MoS_2 membrane described by Heiranian's model in the z-direction. Each membrane is between the two blue-dashed lines along z-direction.

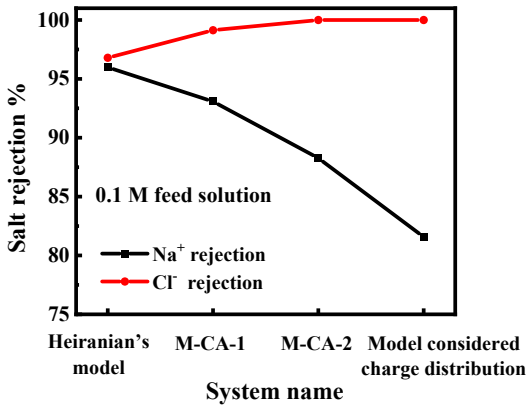

Fig. S5 The change trends of ions rejection rate for Na^+ ions and Cl^- ions in MoS_2 membranes with different atomic charges under 50 MPa and 0.1 M feed solution.

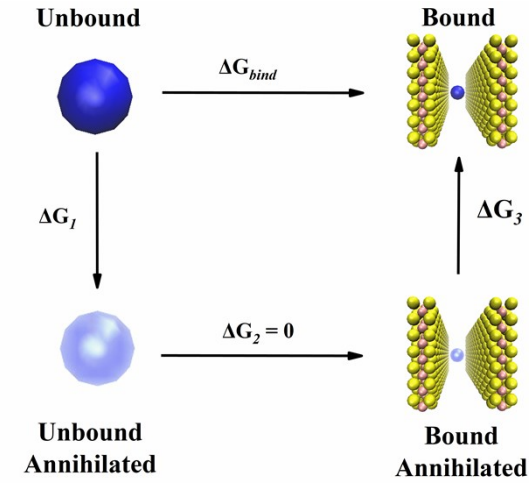

Fig. S6 Schematic diagram of the thermodynamic cycle used to calculate the binding free energy between Na^+/Cl^- ions and MoS_2 nanosheets.

4. Supplementary Tables

Table. S1 The size of the simulation box for MoS_2 membranes with different pore width.

Pore width (nm)	*x*-direction (nm)	*y*-direction (nm)	*z*-direction (nm)
0.6	7.1	6.7	46
0.7	7.1	7.3	46
0.8	7.1	7.9	46
0.9	7.1	8.5	46
1.1	7.1	9.7	46

Table. S2 The number of water molecules, Na^+/Cl^- ions in the simulation system with different pore width.

Pore width (nm)	The number of water molecules in feed solution	The number of water molecules in permeate solution	The number of NaCl in the left box
0.6	10883	5334	98
0.7	11631	5840	106
0.8	12436	6198	112
0.9	13230	6612	120
1.1	15024	7318	135

Table. S3 LJ parameters and atomic charges employed in this work

Atoms	σ (nm)	ε/k_B (kJ/mol)	Charge
C [2]	0.385	0.439	0
S [3, 4]	0.313	1.930	-0.367
Mo [3, 4]	0.420	0.056	0.734
O [5]	0.315	0.636	-0.834
H [5]	0	0	0.417
Na [6]	0.243	0.196	1
Cl [6]	0.356	0.293	-1

Table. S4 The interaction energies of van der Waals interactions and electrostatic interactions between water molecules and MoS_2 nanosheets in different models under 100 MPa.

System name	Interaction energy between water molecules and MoS_2 nanosheets	
	van der Waals interactions (kJ/mol)	electrostatic interactions (kJ/mol)
Heiranian's model	-27324.1 ± 110	0
M-CA-1	-27445.2 ± 110	-3419.74 ± 14
M-CA-2	-27022.3 ± 77	-9758.38 ± 12
Model considered charge distribution	-26624 ± 160	-16155.2 ± 66

Table. S5 The interaction energies (including vdW/ΔG_{vdW}, Coulomb/ΔG_{ele} and total/ΔG_{bind} energies) of Na^+/Cl^- ions in bulk water and in Heiranian's model.

System		Interaction energies (kJ/mol)					
		vdW	ΔG_{vdW}	Coulomb	ΔG_{ele}	Total	ΔG_{bind}
Na^+	in bulk water	1.57	-	-407.33	-	-405.76	-
	in Heiranian's model	1.52	-0.05	-424.26	-16.93	-422.74	-16.98
Cl^-	in bulk water	1.07	-	-363.37	-	-362.30	-
	in Heiranian's model	-2.21	-3.28	-338.70	24.67	-340.91	21.39

References

1. L. Liang, J. C. Li, L. Zhang, Z. Zhang, J. W. Shen, L. Li and J. Wu, *Phys. Chem. Chem. Phys.*, 2017, **19**, 30031-30038.
2. A. D. MacKerell, D. Bashford, M. Bellott, R. L. Dunbrack, J. D. Evanseck, M. J. Field, S. Fischer, J. Gao, H. Guo, S. Ha, D. Joseph-McCarthy, L. Kuchnir, K. Kuczera, F. T. K. Lau, C. Mattos, S. Michnick, T. Ngo, D. T. Nguyen, B. Prodhom, W. E. Reiher, B. Roux, M. Schlenkrich, J. C. Smith, R. Stote, J. Straub, M. Watanabe, J. Wiórkiewicz-Kuczera, D. Yin and M. Karplus, *J. Phys. Chem. B*, 1998, **102**, 3586-3616.

3. A. K. Rappé and W. A. Goddard, *J. Phys. Chem.*, 1991, **95**, 3358-3363.

4. U. Becker, K. M. Rosso, R. Weaver, M. Warren and M. F. Hochella, *Geochim. Cosmochim. Acta*, 2003, **67**, 923-934.

5. J. Liu, G. Shi, P. Guo, J. Yang and H. Fang, *Phys. Rev. Lett.*, 2015, **115**, 164502.

6. Y. Duan, C. Wu, S. Chowdhury, M. C. Lee, G. Xiong, W. Zhang, R. Yang, P. Cieplak, R. Luo, T. Lee, J. Caldwell, J. Wang and P. Kollman, *J. Comput. Chem.*, 2003, **24**, 1999-2012.